Supplementary Information for "Effects of Ligand vs. Linker on Phase Behavior and Mechanical Properties of Nanoparticle Gels"

Qizan Chen,[1] Dinesh Sundaravadivelu Devarajan,[1] Arash Nikoubashman,[2,3] Michael P. Howard,[4,a)] and Jeetain Mittal[1,5,6,b)]

[1)] *Artie McFerrin Department of Chemical Engineering, Texas A&M University, College Station, TX 77843, United States*

[2)] *Leibniz-Institut für Polymerforschung Dresden e.V., Hohe Straße 6, 01069 Dresden, Germany*

[3)] *Institut für Theoretische Physik, Technische Universität Dresden, 01069 Dresden, Germany*

[4)] *Department of Chemical Engineering, Auburn University, Auburn, Alabama 36849, United States*

[5)] *Department of Chemistry, Texas A&M University, College Station, TX 77843, United States*

[6)] *Interdisciplinary Graduate Program in Genetics and Genomics, Texas A&M University, College Station, TX 77843, United States*

[a)]Electronic mail: mphoward@auburn.edu

[b)]Electronic mail: jeetain@tamu.edu

I. SUPPLEMENTARY FIGURES

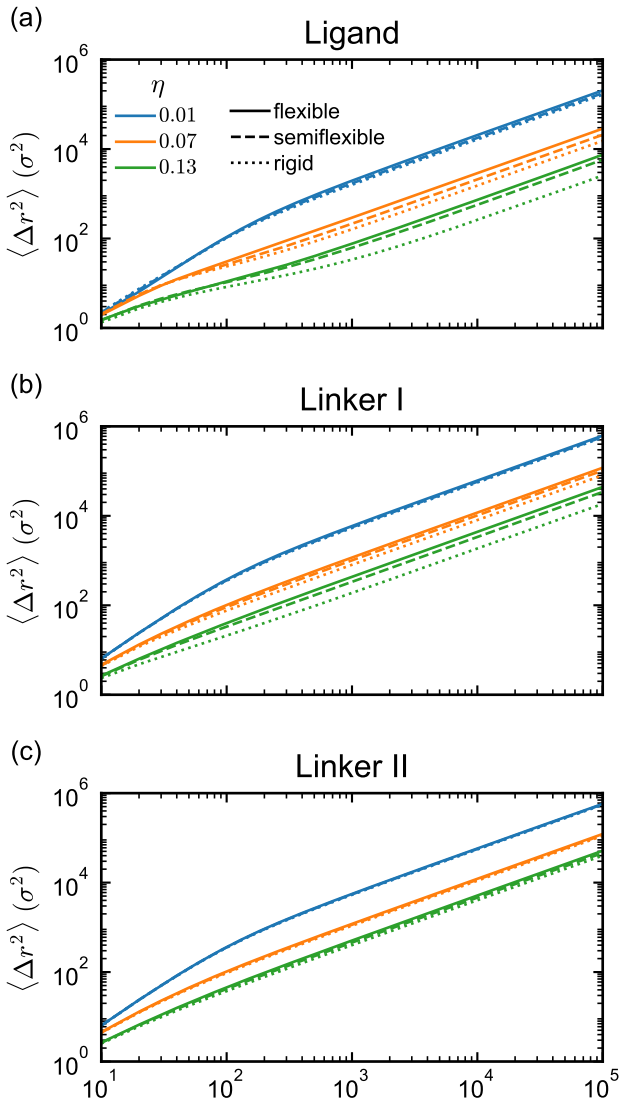

FIG. S1. Mean squared displacement of (a) ligand-, (b) Linker I-, and (c) Linker II-mediated nanoparticles with purely repulsive interactions. Colors indicate different volume fractions η, and line styles represent polymer bending stiffness: solid (flexible), dashed (semiflexible), and dotted (rigid).Simulations were run for $5\times10^5\tau$, starting from the initial dispersed state prior to annealing, with nanoparticle centers saved every 10τ

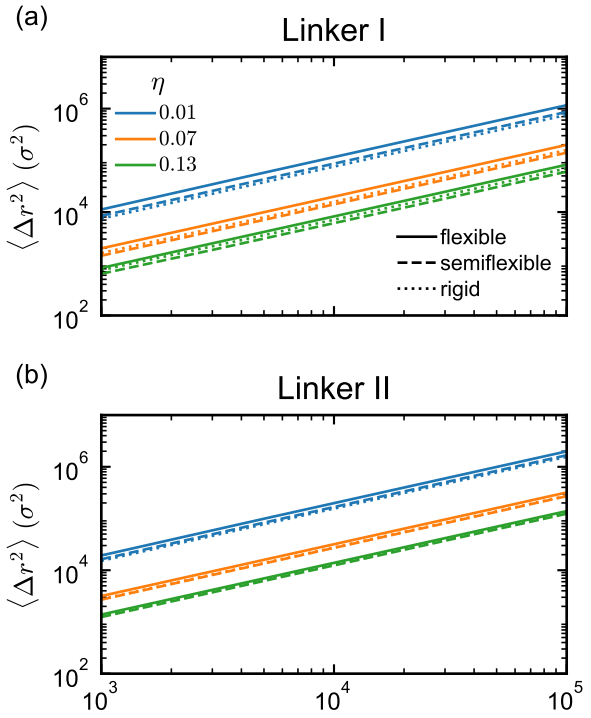

FIG. S2. Mean squared displacement of polymer monomers in (a) Linker I- and (b) Linker II-mediated nanoparticles with purely repulsive interactions. Colors indicate different volume fractions η, and line styles represent polymer bending stiffness: solid (flexible), dashed (semiflexible), and dotted (rigid).The simulations and analysis protocols are identical to those described for Fig. S1; except that polymer monomer positions were saved every $10^3\tau$ to reduce storage demands.

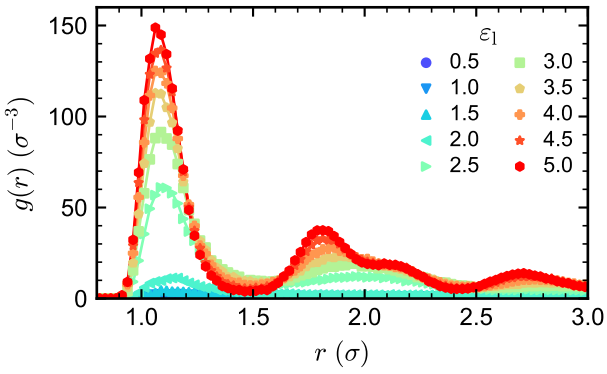

FIG. S3. Radial distribution function between attractive beads of flexible ligands on different nanoparticles as a function of ligand–ligand attraction strength ε_1.

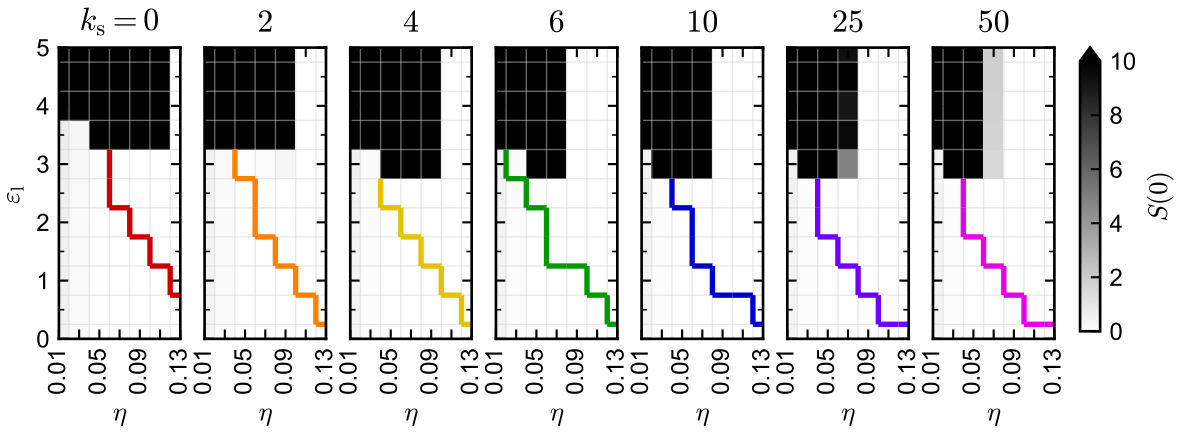

FIG. S4. Nanoparticle partial static structure factor extrapolated to zero wavevector, $S(0)$, and percolation line as a function of volume fraction η and ligand–ligand attraction strength ε_l for different ligand bending stiffnesses k_s.

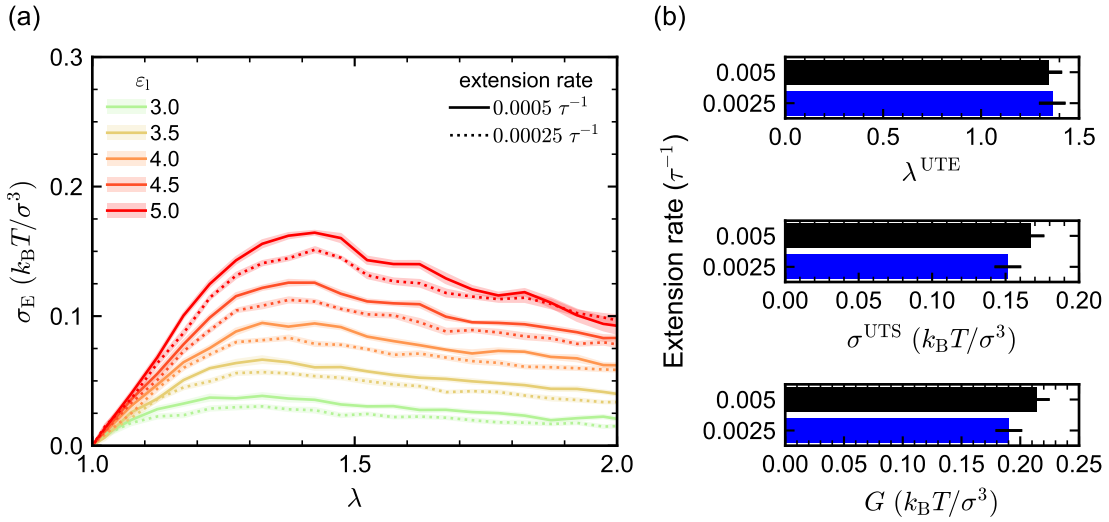

FIG. S5. (a) Engineering stress σ_E as a function of strain λ for semiflexible ligands under two extension rates $0.00025\tau^{-1}$ (dashed lines) and $0.0005\tau^{-1}$ (solid lines). (b) Comparison of mechanical properties λ^{UTE}, σ^{UTS}, and G for $\varepsilon_l = 5$ at the two extension rates. Error bars represent the standard error of the mean across independent simulations and extension directions.

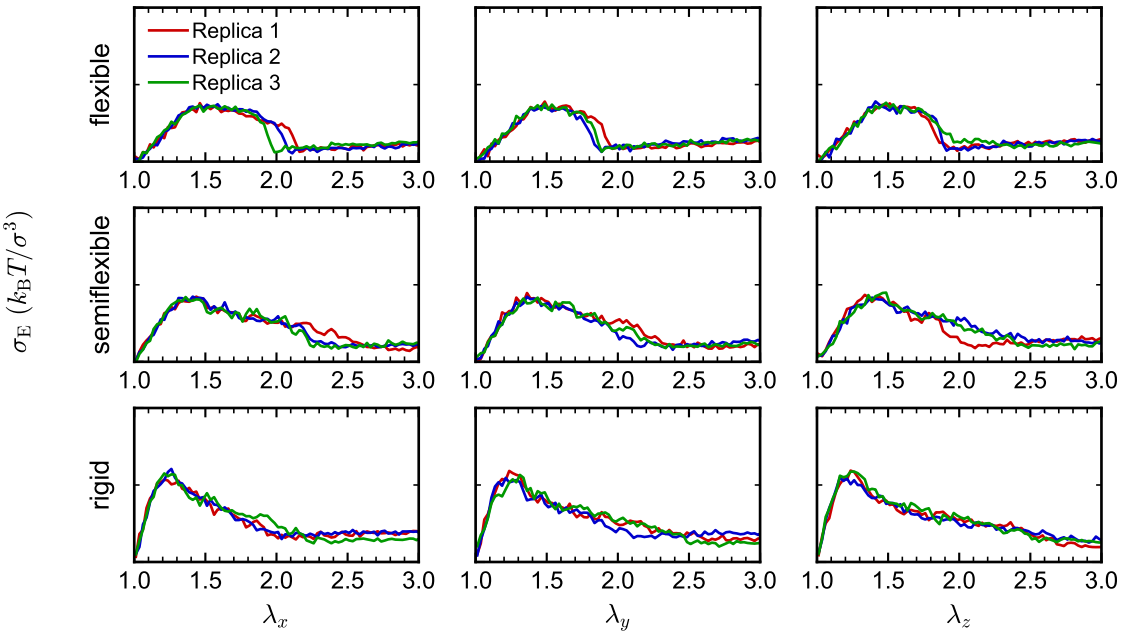

FIG. S6. Engineering stress σ_E for ligand-mediated nanoparticle assemblies under uniaxial tensile deformation (extension factor λ) in three different stretching directions and three independent simulations for flexible, semiflexible, and rigid ligands.

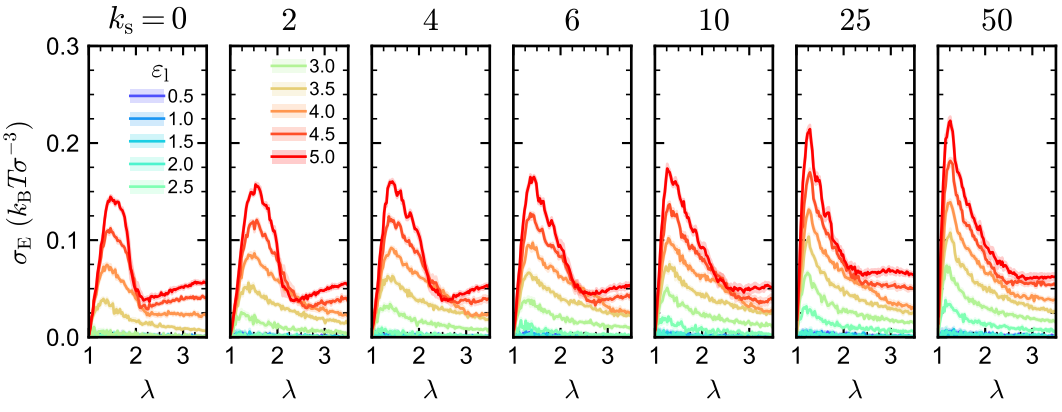

FIG. S7. Engineering stress σ_E for ligand-mediated nanoparticle assemblies under uniaxial tensile deformation (extension factor λ) for different ligand bending stiffnesses k_s. Error bars represent the standard error of the mean across independent simulations and extension directions.

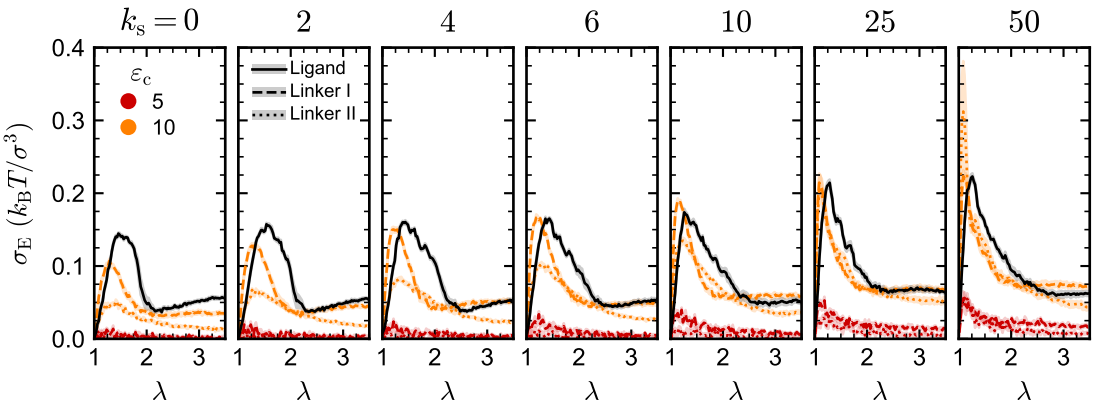

FIG. S8. Engineering stress σ_E of Linker I- (dashed lines) and Linker II- (dotted lines) mediated nanoparticle assemblies to uniaxial tensile deformation (extension factor λ) at a fixed linker–linker attraction strength $\varepsilon_l = 5$ and two different linker–nanoparticle attraction strengths ε_c for different linker bending stiffnesses k_s. The solid lines show the same measurements for the ligand-mediated nanoparticle assemblies with ligand–ligand attraction strength $\varepsilon_l = 5$. Error bars represent the standard error of the mean across independent simulations and extension directions.

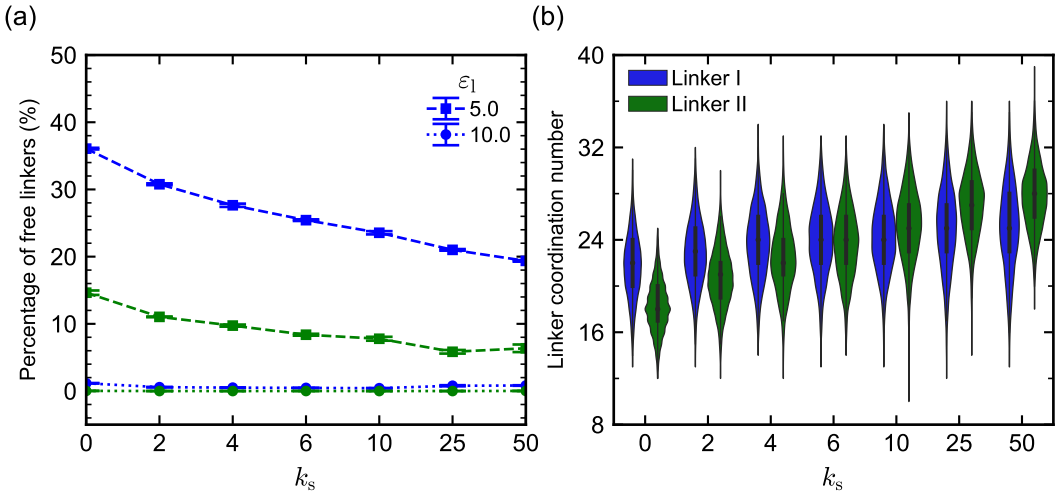

FIG. S9. (a) Percentage of free linkers as a function of polymer bending stiffness k_s for Linker I- (blue) and Linker II- (green) mediated nanoparticle assemblies with $\eta = 0.13$, $\varepsilon_l = 5$, and varied $\varepsilon_c = 5$ or 10. Error bars represent the standard error of the mean across the final assemblies from annealing. (b) Corresponding violin plot of linker coordination number per nanoparticle at $\varepsilon_c = 10$.

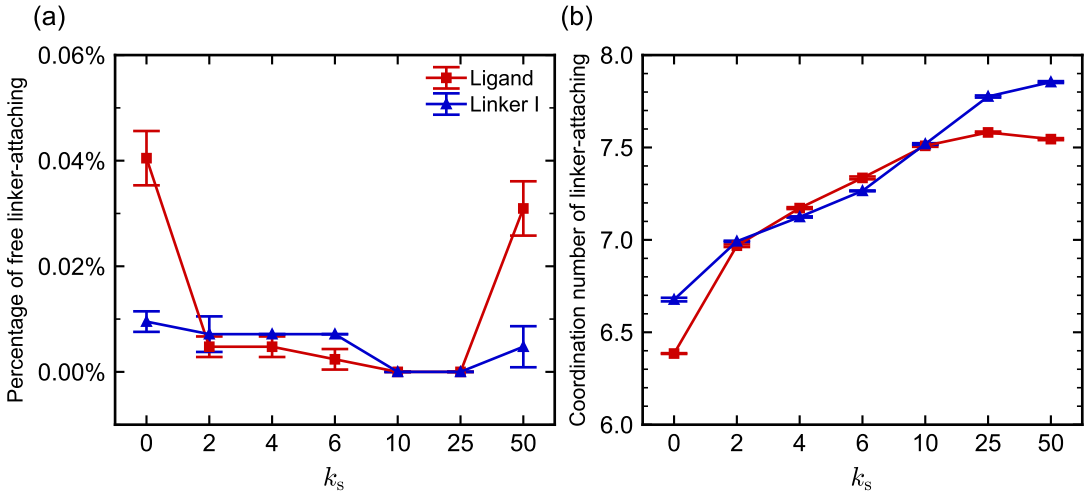

FIG. S10. (a) Percentage of free linker-attaching beads and (b) averaged linker-attaching coordination number as a function of polymer bending stiffness k_s for ligand- (red) and Linker I- (blue) mediated nanoparticle assemblies with $\eta = 0.13$, $\varepsilon_l = 5$ and $\varepsilon_c = 10$. Error bars represent the standard error of the mean across the final assemblies from annealing.

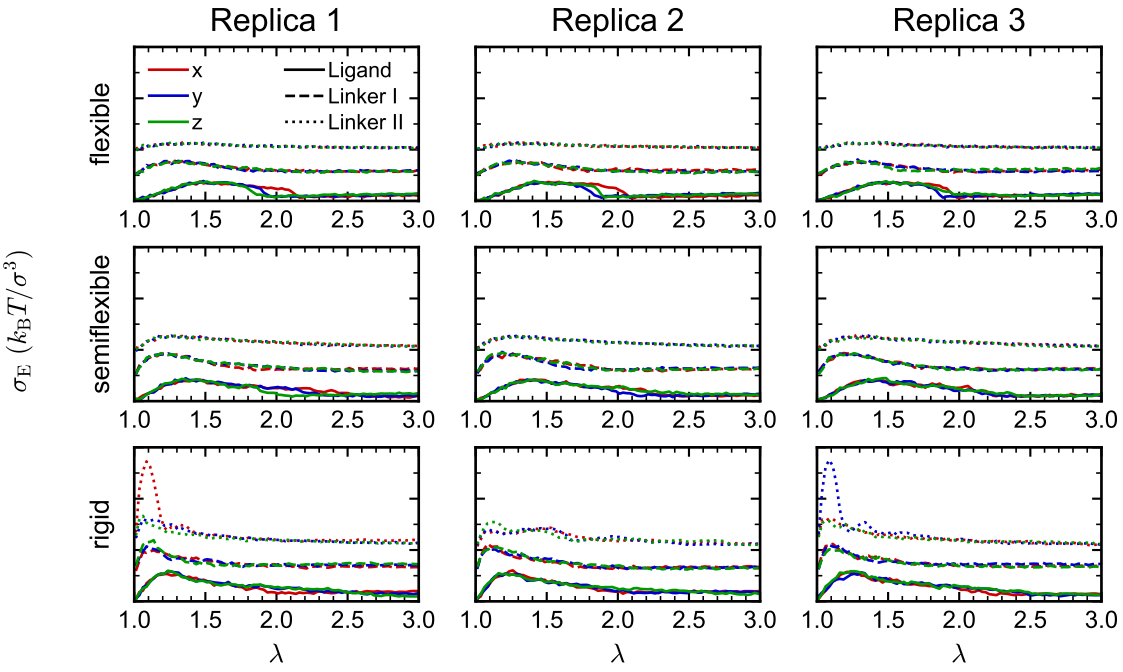

FIG. S11. Engineering stress σ_E as a function of the extension factor λ in the x, y, and z directions for ligand- (solid Line), Linker I- (dashed Line), and Linker II- (dotted Line) mediated nanoparticle assemblies using flexible, semiflexible, and rigid polymers. Results are shown for three independent simulations.

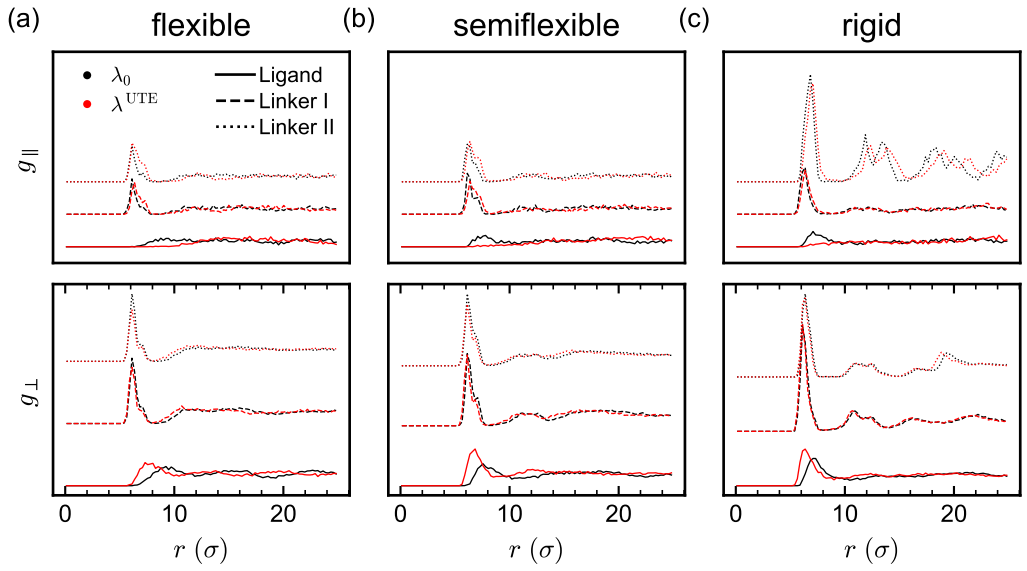

FIG. S12. Nanoparticle–nanoparticle radial distribution function parallel $g_{||}$ and perpendicular $g_{\perp}$ to the direction of deformation for (a) flexible, (b) semiflexible, and (c) rigid ligand, Linker I and Linker II polymers. The black and red lines correspond to systems before ($\lambda = 0$) and after deforming to $\lambda = \lambda^{\mathrm{UTE}}$, respectively. The calculation was done following the methodology described in Ref. 7.

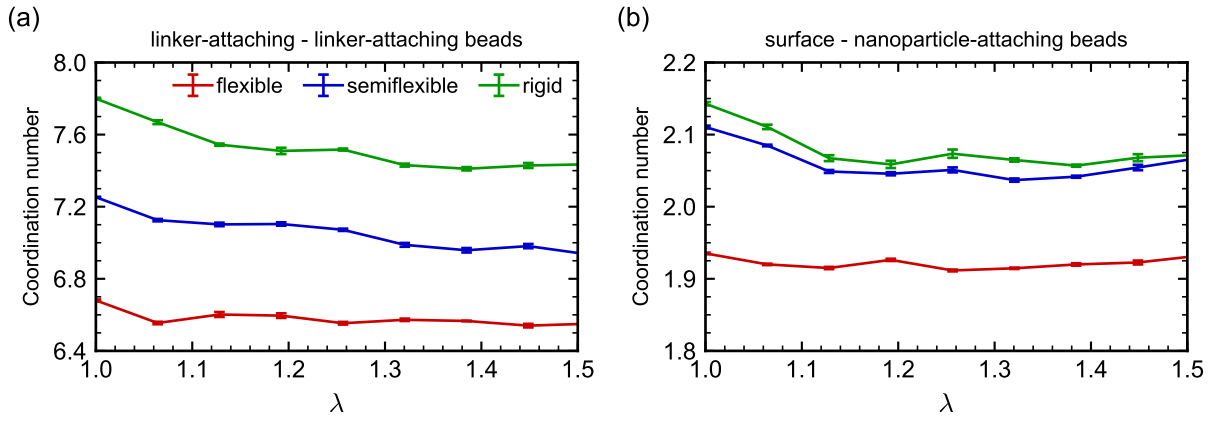

FIG. S13. Coordination number of beads as a function of the extension factor λ for flexible, semiflexible and rigid Linker I-mediated nanoparticle assemblies with $\varepsilon_{\mathrm{l}} = 5$ and $\varepsilon_{\mathrm{c}} = 10$. (a) Coordination number between linker-attaching beads. (b) Coordination number between surface and nanoparticle-attaching beads. Error bars represent the standard error of the mean across independent simulations and extension directions.

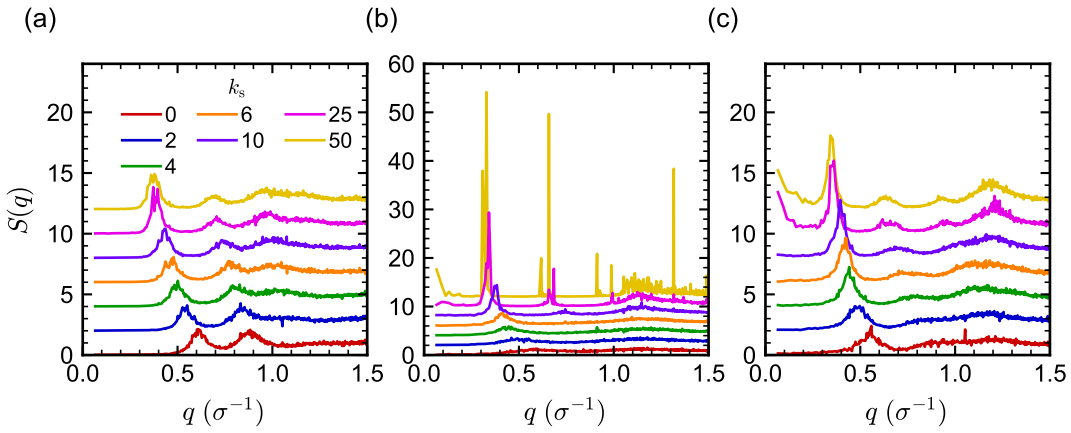

FIG. S14. Nanoparticle partial static structure factor $S(q)$ for different bending stiffnesses k_s: (a) ligand-mediated nanoparticle assemblies with ligand–ligand attraction strength $\varepsilon_l = 5$, (b) Linker I-mediated nanoparticle assemblies with linker–linker attraction strength $\varepsilon_l = 5$ and linker–nanoparticle attraction strength $\varepsilon_c = 10$, and (c) Linker II-mediated nanoparticle assemblies with linker–nanoparticle attraction strength $\varepsilon_c = 10$. The data lines are additionally offset by 2 in order from smallest to largest k_s to better compare the differences.

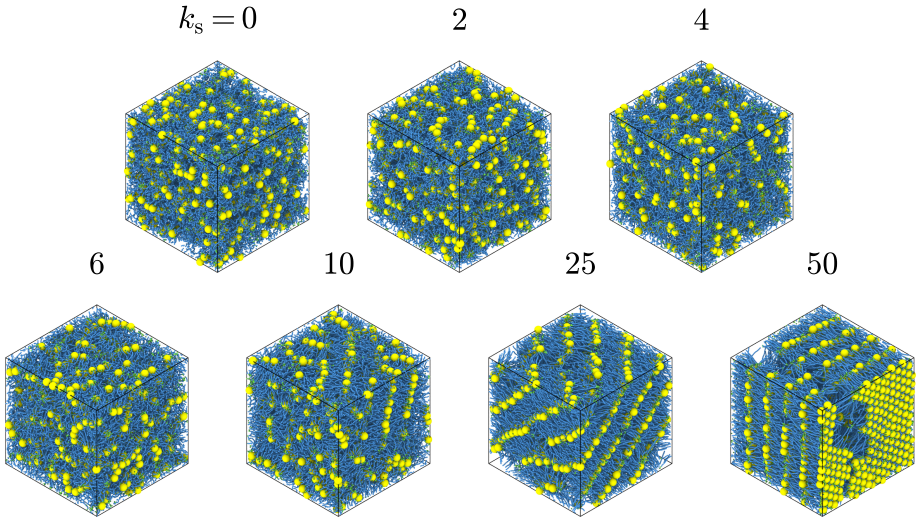

FIG. S15. Simulation snapshots of Linker II-mediated nanoparticle assemblies with a fixed linker–nanoparticle attraction strength $\varepsilon_c = 10$ for all bending stiffnesses k_s investigated.

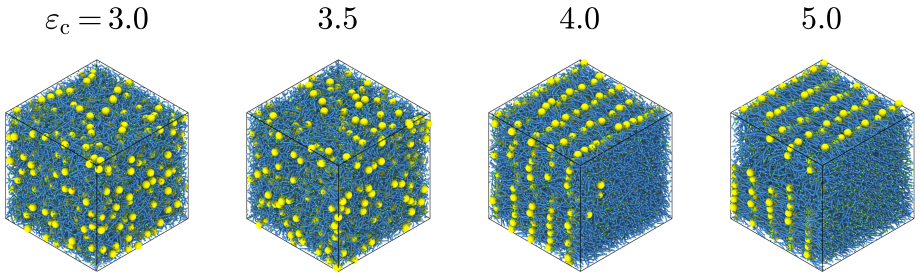

FIG. S16. Simulation snapshots of Linker II-mediated nanoparticle assemblies with fixed bending stiffness $k_s = 50$ as a function of linker–nanoparticle attraction strength ε_c.

II. SUPPLEMENTARY MOVIES

- Movie S1. Uniaxial tensile deformation of flexible ligand-mediated nanoparticle assembly for ligand–ligand attraction strength $\varepsilon_{\mathrm{l}} = 5$.
- Movie S2. Uniaxial tensile deformation of semiflexible ligand-mediated nanoparticle assembly for ligand–ligand attraction strength $\varepsilon_{\mathrm{l}} = 5$.
- Movie S3. Uniaxial tensile deformation of rigid ligand-mediated nanoparticle assembly for ligand–ligand attraction strength $\varepsilon_{\mathrm{l}} = 5$.
- Movie S4. Uniaxial tensile deformation of flexible Linker I-mediated nanoparticle assembly for linker–linker attraction strength $\varepsilon_{\mathrm{l}} = 5$ and linker–nanoparticle attraction strength $\varepsilon_{\mathrm{c}} = 10$.
- Movie S5. Uniaxial tensile deformation of semiflexible Linker I-mediated nanoparticle assembly for linker–linker attraction strength $\varepsilon_{\mathrm{l}} = 5$ and linker–nanoparticle attraction strength $\varepsilon_{\mathrm{c}} = 10$.
- Movie S6. Uniaxial tensile deformation of rigid Linker I-mediated nanoparticle assembly for linker–linker attraction strength $\varepsilon_{\mathrm{l}} = 5$ and linker–nanoparticle attraction strength $\varepsilon_{\mathrm{c}} = 10$.
- Movie S7. Uniaxial tensile deformation of flexible Linker II-mediated nanoparticle assembly for linker–nanoparticle attraction strength $\varepsilon_{\mathrm{c}} = 10$.
- Movie S8. Uniaxial tensile simulation of semiflexible Linker II-mediated nanoparticle assembly for linker–nanoparticle attraction strength $\varepsilon_{\mathrm{c}} = 10$.
- Movie S9. Uniaxial tensile deformation of rigid Linker II-mediated nanoparticle assembly for linker–nanoparticle attraction strength $\varepsilon_{\mathrm{c}} = 10$.